

## Use of RNA Interference and Complementation To Study the Function of the *Drosophila* and Human 26S Proteasome Subunit S13

Josefin Lundgren,<sup>1</sup> Patrick Masson,<sup>1</sup> Claudio A. Realini,<sup>2</sup> and Patrick Young<sup>1\*</sup>

Department of Molecular Biology, Stockholm University, Stockholm, Sweden,<sup>1</sup> and Oncology Institute of Southern Switzerland, Laboratory of Experimental Oncology, Bellinzona, Switzerland<sup>2</sup>

Received 27 January 2003/Returned for modification 10 March 2003/Accepted 29 April 2003

**The S13 subunit (also called Pad1, Rpn11, and MPR1) is a component of the 19S complex, a regulatory complex essential for the ubiquitin-dependent proteolytic activity of the 26S proteasome. To address the functional role of S13, we combined double-stranded RNA interference (RNAi) against the *Drosophila* proteasome subunit DmS13 with expression of wild-type and mutant forms of the homologous human gene, HS13. These studies show that DmS13 is essential for 26S function. Loss of the S13 subunit in metazoan cells leads to increased levels of ubiquitin conjugates, cell cycle defects, DNA overreplication, and apoptosis. In vivo assays using short-lived proteasome substrates confirmed that the 26S ubiquitin-dependent degradation pathway is compromised in S13-depleted cells. In complementation experiments using *Drosophila* cell lines expressing HS13, wild-type HS13 was found to fully rescue the knockdown phenotype after DmS13 RNAi treatment, while an HS13 containing mutations (H113A-H115A) in the proposed isopeptidase active site was unable to rescue. A mutation within the conserved MPN/JAMM domain (C120A) abolished the ability of HS13 to rescue the *Drosophila* cells from apoptosis or DNA overreplication. However, the C120A mutant was found to partially restore normal levels of ubiquitin conjugates. The S13 subunit may possess multiple functions, including a deubiquitylating activity and distinct activities essential for cell cycle progression that require the conserved C120 residue.**

The ubiquitin-proteasome system is the major nonlysosomal pathway responsible for the degradation of intracellular proteins in eukaryotic cells. This system participates in the regulation of a vast number of cellular pathways through timely and specific conjugation of target proteins with multiple ubiquitin molecules followed by proteolysis by the 26S proteasome (52). The 26S proteasome is a large protease (2,500 kDa) composed of a 20S catalytic core and a 19S regulatory complex that associates with the ends of the 20S proteasome in an ATP-dependent manner. The 20S core (700 kDa) is a compartmentalized multicatalytic complex composed of a total of 28  $\alpha$  and  $\beta$  subunits arranged in four stacked heptameric rings. The subunits generate a hollow cylindrical structure that separates the cytosolic environment from the catalytic sites located at the luminal face of the  $\beta$ -rings (16, 30, 46, 60). In the absence of regulatory factors, the 20S proteasome exists in an autoinhibited (latent) state in which the free N-terminal tails of its  $\alpha$  subunits extend into the 20S pores and thus sterically block substrate access to the lumen (17). Activation of the 20S proteasome requires interactions of the  $\alpha$  subunits with specific regulators, such as the PA28 $\alpha\beta$  or  $\gamma$  heptamer (35), PA200 (47), or the 19S regulatory complex (8).

The 19S complex has been directly implicated in nonproteolytic regulatory functions, such as nucleotide excision-repair (10, 38) and transcription elongation (7, 14). Its main function however, is to carry out several distinct steps critical for ubiquitin-dependent proteolysis by 26S (8). First, the 19S complex

acquires ubiquitylated substrates and recycles the ubiquitin chains once substrate degradation has been initiated (19, 22). Second, it promotes substrate unfolding required for translocation into the proteolytic chamber (3). Third, 19S interacts with the  $\alpha$ -ring of the 20S proteasome and mediates conformational changes necessary for gating and, presumably, activation of the proteasome's active sites (13).

In vitro interaction analyses and structural studies have shed some light on the topographical arrangements of the 19S subunits (9, 13, 15, 53) and have identified two structurally and functionally distinct subcomplexes: the base and the lid. The base includes the six ATPase subunits involved in substrate anchoring and unfolding and in the gating of the 20S pore. The lid contains eight subunits necessary for the processing of polyubiquitylated proteins and exhibiting striking homology to the COP9-signalosome complex and eIF3 (12).

At the functional level, studies have focused mainly on the aspect of ubiquitin binding, identifying subunits S5a (also called p54 and Rpn10) and S6' as ubiquitin chain acceptors (18, 25, 49, 59). Another aspect, the removal of the ubiquitin chains following substrate binding, has only recently been addressed. Although little is known about the contributions of individual subunits, these deubiquitylating activities are thought to be essential for 26S-dependent protein degradation (54), and they have been detected in 19S particles of yeast and *Drosophila* (21, 26–28).

In this work, we examine the function of S13 (also called Rpn11, pad1, Mpr1, and CepP1), a highly conserved subunit of the 19S complex. Similar to other 19S subunits, mutations of yeast S13 result in increased pools of ubiquitylated proteins, cell cycle arrests, and resistance to methyl 2-benzimidazolecarbamate (33, 36). In addition, S13 mutations generate a wider

\* Corresponding author. Mailing address: Department of Molecular Biology and Functional Genomics, Stockholm University, S-10691 Stockholm, Sweden. Phone: 46-8-164135. Fax: 46-8-152350. E-mail: patrick.young@molbio.su.se.

range of phenotypes, including overreplication of nuclear and mitochondrial DNA (36, 37), but unlike that of other subunits, S13 overexpression also resulted in broad multidrug resistance against a variety of unrelated drugs (1, 43, 48).

S13 and Csn5 were recently included in a large family of isopeptidases that share the unique JAMM isopeptidase active site (5, 51, 58). While the majority of previously identified isopeptidases contain thiol active sites, metal chelator studies and site-directed mutagenesis of the yeast S13 (Rpn11) subunit indicate that the JAMM isopeptidase is not a thiol protease but instead is a novel zinc metalloprotease. Alignment of the JAMM isopeptidase family members and the identification of conserved residues in a putative catalytic MPN subdomain (MPN+) of S13 and Csn5 (31) highlight the strict conservation of the proposed zinc binding residues and support the enzymatic functions of yeast S13, Rpn11. The S13 and Csn5 subunits also share an additional conserved domain, GCWLS, which is embedded within the JAMM isopeptidase motif. This motif is unique to S13 and Csn5, as it is absent in all other JAMM proteins, and is reminiscent of the Cys box of ubiquitin hydrolases (11).

To study the largely uncharacterized metazoan S13, we have developed a new approach that we call RNAi+c. This new technique combines simultaneous double-stranded RNA (dsRNA) interference (RNAi) with complementation (c) by expression of a homologous gene under the control of an inducible promoter. In a series of RNAi+c studies, we used RNAi to remove the endogenous *Drosophila* S13 (DmS13) in Schneider 2 (S2) cell lines expressing the wild-type or mutant form of human S13 (HS13). In the absence of HS13, DmS13 RNAi results in accumulation of polyubiquitinated species, DNA overreplication, cell cycle block, and apoptosis. As expected, complementation with wild-type HS13 normalizes ubiquitin conjugate pool levels and cell cycle progression, indicating that DmS13 and HS13 are functional homologs. On the other hand, mutations in the proposed isopeptidase active site (H113A-H115A) or a C-terminally truncated HS13 mutant was unable to rescue any depletion phenotypes. Finally, an HS13 containing a Cys-to-Ala mutation within the conserved GCWLS sequence rescued only a subset of the DmS13 RNAi phenotypes in metazoan cells. Our results indicate that metazoan S13 is a highly conserved protein essential for 26S proteasome activity and that this subunit may also participate in additional cellular functions not directly associated with protein degradation.

#### MATERIALS AND METHODS

**Chemical reagents and antibodies.** Rabbit polyclonal antibodies against a sodium dodecyl sulfate-polyacrylamide gel electrophoresis (SDS-PAGE)-purified recombinant *Drosophila* S5a subunit were generated by Agrisera. Antibodies against proteasome subunit  $\alpha 7$  (HC8), ubiquitin, and the proteasome inhibitor MG132 were from AFFINITI. Horseradish peroxidase-conjugated secondary antibodies and the ECL+ detection kit were from Amersham Biosciences. Hygromycin was purchased from Invitrogen.

**Cell culture.** S2 cells were cultured in Schneider's *Drosophila* medium (Gibco) supplemented with 10% fetal calf serum, 50 U of penicillin/ml, 50  $\mu$ g of streptomycin/ml, and 2 mM L-glutamine. The cells were maintained at 24°C and passed every 7 days at a 1:4 dilution.

**Stable cell lines.** For constitutive expression in *Drosophila* S2 cells, the genes for the short-lived green fluorescent proteins (GFP) Ub<sup>G76V</sup>GFP and Ub-R-GFP (6) were subcloned into the pAct vectors (Invitrogen). The human wild-type and mutant S13 genes were subcloned into the CuSO<sub>4</sub>-inducible vector pMT/

V5-hisA containing the metallothionein promoter. Stable *Drosophila* S2 cell clones were isolated according to the manufacturer's protocols. Briefly,  $3 \times 10^6$  S2 cells were transfected using calcium phosphate. The amounts of DNA added to each transfection were as follows: selection plasmid (PCoHYGRO), 5  $\mu$ g; specific plasmid (e.g., S13 or short-lived GFP), 15  $\mu$ g. Five days after transfection, the cells were selected for by the addition of 300  $\mu$ g of hygromycin/ml. Stable cell lines were expanded after 3 weeks and maintained in the presence of hygromycin (300  $\mu$ g/ml). Expression of the S13 gene products was confirmed by induction at different CuSO<sub>4</sub> concentrations followed by Western blotting.

**A metalloisopeptidase active-site S13 mutant.** Site-directed mutagenesis (H113A and H115A) was carried out to generate specific mutations in the proposed metalloisopeptidase active site of HS13 (51, 58). The mutagenesis was performed using the Stratagene Quick-Change site-directed mutagenesis kit on the wild-type HS13 gene in a pMT/V5-hisA expression vector. The two primers used for mutagenesis were 5'-GGTTGGTTGGTATGCCAGTGCACCTGCTTTGGTTGTTGGC-3' and 5'-GCCAACAACCAAGCCAGGTGCACTGGCATACCAACCAACAACC-3'. The resulting mutant construct was confirmed by sequencing, and a stable cell line was generated in *Drosophila* S2 cells.

**dsRNA synthesis.** For the RNAi experiments, dsRNA was synthesized with the aid of the MEGAscript kit (Ambion). *Drosophila* genomic DNA was isolated from wild-type Oregon *Drosophila* using the DNaseasy tissue kit from Qiagen. Oligonucleotides were selected by searching the GadFly database. The selected oligonucleotides amplified within the largest exon of the *Drosophila* S13 gene. PCR of *Drosophila* genomic DNA was performed to create a 700-bp fragment of the second exon region of S13 with the following primers: 5'-CTGCTACGCTTGGAGGTGCTATGCCACAGG-3' and 5'-ACAGTGCTCATTGTAGTCGACAACGTGAGGC-3'. A second set of primers was used to introduce a T7 RNA polymerase binding site on the 700-bp fragment: 5'-GAATTAATACGACTCACTATAGGGGAGACTGCTACGCTTGGAGGTGCTATGC-3' and 5'-GAATTAATACGACTCACTATAGGGGAGAAACAGTGTCTATTGTAGTCGGACAAC-3'. The S5a T7-tailed DNA was produced by PCR amplification of a clone in a pET26b vector with the following primers: 5'-GAATTAATACGACTCACTATAGGGGAGACGCGCTTAATGGCAAGGACG-3' and 5'-GAATTAAATACGACTCACTATAGGGGAGAGCGAGTCCTTGGCCGTCGCTC-3'.

GFP T7-tailed DNA was produced with PCR amplification from recombinant GFP with the following primers: 5'-GAATTAATACGACTCACTATAGGGGAGA-3' and 5'-GAATTAATACGACTCACTATAGGGGAGAAATGCCGAGAGTGATCCCGCGCGCGG-3'. The dsRNA was purified with the RNAeasy kit (Qiagen), followed by annealing (in 0.1 M NaCl plus 20 mM Na citrate [pH 6.8] buffer) for 30 min at 65°C, followed by slow cooling to room temperature.

**RNAi+c.** RNAi treatment of *Drosophila* S2 cells was performed essentially as previously described (4). Briefly, 3 ml of S2 cell cultures was plated at a concentration of  $10^6$  cells/ml in Schneider's *Drosophila* medium. After cell attachment, the medium was replaced with 1 ml of DES serum-free medium (Invitrogen). To initiate RNAi, 30  $\mu$ g of dsRNA was added directly to the medium under constant agitation. After 6 to 16 h, 2 ml of Schneider's medium containing 10% fetal bovine serum was added, and the cells were cultured for 3 to 4 days prior to analysis. For complementation studies in DmS13 RNAi-treated cells, expression of wild-type and mutant HS13 from the inducible metallothionein promoter was initiated by addition of CuSO<sub>4</sub> together with the serum-containing medium. In dose-response experiments followed by Western blot analysis, we determined that at a concentration of 300  $\mu$ M CuSO<sub>4</sub>, S2 cells were expressing significant amounts of the HS13s without noticeable toxic effects or interference with ubiquitin metabolism.

**Flow cytometry.** For cell cycle analysis, *Drosophila* S2 cells were processed using a bromodeoxyuridine (BrdU) flow kit (BD PharMingen). For detection of newly synthesized DNA, DmS13 RNAi-treated S2 cells ( $3 \times 10^6$ ) were incubated for 4 h in medium containing the thymidine analog BrdU (20  $\mu$ M). Total DNA was detected by staining with 7-amino-actinomycin D (7-AAD) according to the BD PharMingen BrdU flow kit manual. Fluorescence was measured using a FACScan flow cytometer (Becton Dickinson), while data collection and analysis were performed using CellQuest software. To help confirm that the sub-G<sub>0</sub> fraction of S2 cells used in the RNAi+c experiments were apoptotic, we used a control S2 population in which apoptosis was induced with staurosporine. The apoptotic cells induced by staurosporine gave fluorescence-activated cell sorter (FACS) sub-G<sub>0</sub> values identical to those observed in RNAi+c experiments.

**Native gels.** *Drosophila* S2 cells were pelleted, washed with phosphate-buffered saline (PBS), and completely dissolved in buffer (20 mM MOPS [morpholinepropanesulfonic acid], pH 7.5, 20 mM NaAc, 20 mM KCl, 10 mM NaCl, 2 mM MgCl<sub>2</sub>, 1 mM dithiothreitol) containing 4 mM ATP. The cells were lysed by two rapid freeze-thaws using liquid nitrogen. The lysates were cleared by centrifugation at 21,000  $\times g$  for 10 min, and the protein concentrations in the supernatants were determined using the Bradford assay. Cell extracts (100 to 150  $\mu$ g)

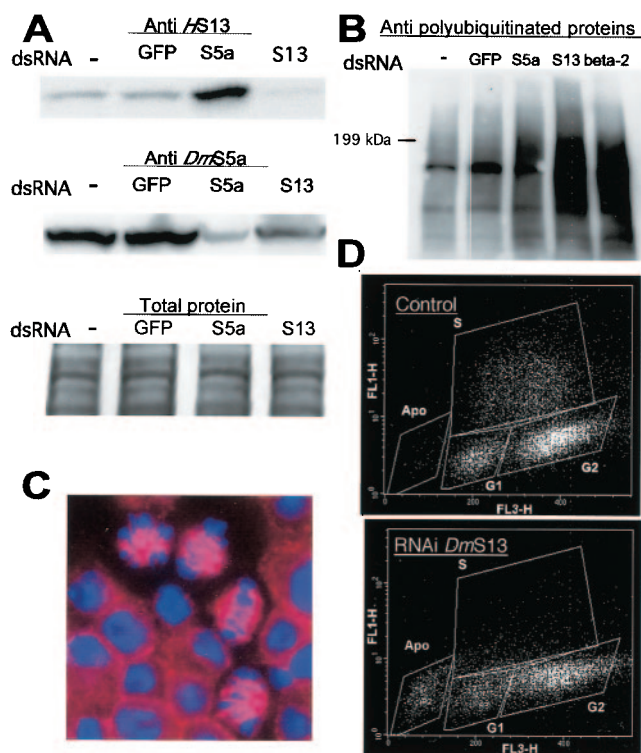


FIG. 1. (A) Western blots showing RNAi knockdown of DmS13 and DmS5a in *Drosophila* S2 cells (top and middle, respectively). Control cells were untreated (–) or exposed to GFP dsRNA. RNAi against DmS5a leads to increased levels of DmS13. To confirm that equivalent amounts of total protein were present in each lane, the Western blots were Coomassie stained after Western detection (bottom). (B) Western blot of S2 cells exposed to dsRNA against DmS13 or DmS5a and probed with ubiquitin chain antibodies. The lane marked with a minus contains lysate from untreated cells. The cells were treated with dsRNA against GFP as a negative control and with dsRNA to the Prosβ2 20S proteasome subunit as a positive control. (C) Immunofluorescence image of S2 cells exposed to dsRNA against DmS13. The cells were fixed, permeabilized, and then stained for  $\alpha$ -tubulin (red) and DNA (blue; DAPI). (D) Cell cycle arrest in *Drosophila* S2 cells treated with dsRNA against the proteasome subunit S13. The cells were labeled with BrdU to measure newly synthesized DNA (y axis) and stained with 7-AAD (x axis) for total cellular DNA.

were loaded onto native gels (3% stacking gel and 4.5% resolving gel) containing 2.25% sucrose. The gels were run at 60 to 80 V for 6 h at 4°C, with Tris-borate-EDTA as the electrophoresis buffer. The Tris-borate-EDTA buffer was replenished one time during the electrophoresis run. After being soaked in distilled water, the gels were overlaid with 500  $\mu$ l of 800  $\mu$ M Suc-Leu-Leu-Val-Tyr-7-amido-4-methylcoumarin (LLVY-MCA) in buffer (30 mM Tris, pH 7.8, 5 mM MgCl<sub>2</sub>, 10 mM KCl, 0.5 mM EDTA). After a 10-min incubation, a total of 600  $\mu$ l of 1% SDS was overlaid on the gel, and the hydrolyzed peptide was visualized using a Bio-Rad UV camera system. To detect incorporated HS13 protein, the visualized 26S bands were excised, soaked in SDS buffer, and run on a gradient gel (Bio-Rad) under denaturing conditions, followed by immunoblotting with anti-S13 antibodies.

**Immunofluorescence staining and assessment of the mitotic index.** S2 cells were plated on Permax chamber slides 3 days after RNAi treatment with Schneider's *Drosophila* medium. The cells were washed with PBS buffer and fixed for 15 min in 3.7% paraformaldehyde. After three washes in PBS, the cells were permeabilized with 0.2% Triton X-100 for 2 min. Following three washes with PBS, the cells were stored in PBS at 4°C until they were stained. Anti-tubulin antibodies were used to stain microtubules, while DAPI (4',6-diamidino-2-phenylindole) was added at 1.5  $\mu$ l/ml in Vectashield (Vector-1000) directly to the cells on the slide. Cells that displayed condensed chromosomes and attached

mitotic spindles were counted as mitotic and divided by the number of total cells present in a viewing field.

## RESULTS

**RNAi-mediated inhibition of S13 and S5a and accumulation of polyubiquitinated proteins.** Previous studies of yeast indicated that S13 (Rpn11 or pad1) is essential for proteasome function and cell viability, while the loss of subunit S5a (Rpn10 or pus1) produced only limited defects in growth and proteolysis (50, 56). Here, we used RNAi to compare the effects of removing the *Drosophila* homologs of S5a (DmS5a) and of S13 (DmS13) from S2 cells. As controls, we performed RNAi against the essential catalytic 20S subunit  $\beta$ 2, Pros $\beta$ 2, and nonspecific RNAi against GFP. After 4 days of RNAi-mediated inhibition, the levels of DmS13 and DmS5a protein were greatly reduced, as shown by Western blot analysis (Fig. 1A), while the levels of both 19S subunits were unaffected by dsRNA directed against GFP. RNAi-mediated inhibition of DmS5a led to a pronounced increase in the DmS13 protein levels (Fig. 1A, top row).

To test the effects of DmS13 and DmS5a depletion on ubiquitinylation, we immunoblotted whole-cell lysates from treated and control cells with anti-polyubiquitin antibodies. The RNAi-mediated inhibition of either DmS5a or DmS13 resulted in the accumulation of high-molecular-weight ubiquitin-conjugated proteins (Fig. 1B). Compared to untreated controls or GFP RNAi-treated cells, the loss of DmS5a led to only a modest increase in ubiquitin conjugates. The removal of DmS13, however, created a large expansion of polyubiquitinated proteins equal to that observed in the RNAi-mediated inhibition of the 20S Pros $\beta$ 2 subunit. Catalytic 20S subunits are essential for proteasome structure and function, and fluorogenic assays confirmed a nearly complete loss of 20S activity after RNAi-mediated inhibition of Pros $\beta$ 2 in S2 cells (data not shown). These results indicate that our approach selectively depleted cells of DmS13 and that the specific loss of DmS13 was responsible for a large increase in polyubiquitin conjugates, comparable to complete disruption of proteasome function.

To assess the effects of the DmS13 knockdown on cell cycle progression, we performed flow cytometry analysis on RNAi-treated S2 cells incubated with BrdU to label newly synthesized DNA. The results shown in Fig. 1D indicate that RNAi treatment against DmS13 led to cell cycle arrest followed by cell death, as indicated by the marked decrease in the S-phase population and the emergence of cells in the sub-G<sub>0</sub> region of the plot. In line with the limited defects observed in ubiquitin metabolism, knockdown of the DmS5a subunit did not significantly increase cell mortality or change cell cycle patterns (data not shown).

To determine at what stage the cell cycle was blocked by DmS13 loss, we carried out fluorescence microscopy analysis of the mitotic patterns. This analysis revealed that, compared to controls or DmS5a RNAi-treated cells, S2 cells depleted of DmS13 reproducibly exhibited two- to threefold-higher frequencies of condensed chromosomes and attached mitotic spindles, a pattern indicative of metaphase arrest (Fig. 1C). In good agreement with previous reports of the effects of S13 mutations in yeast (33), ~10 to 15% of the cells exhibited

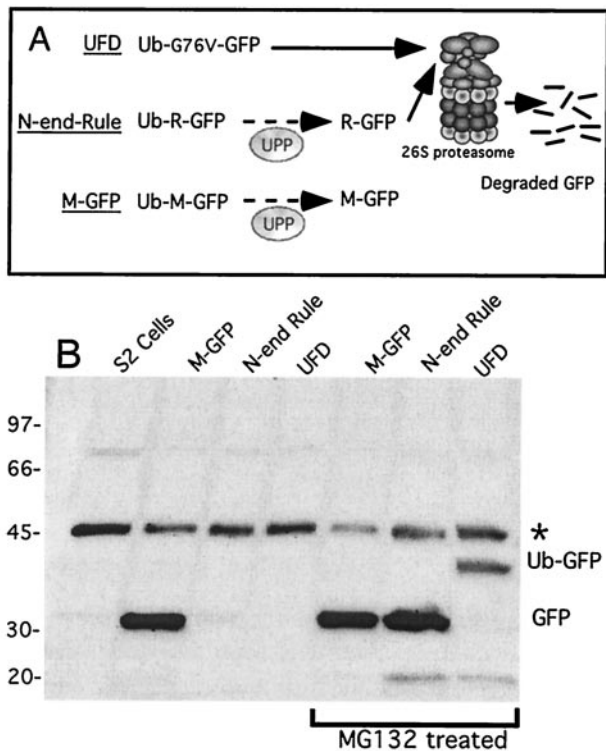


FIG. 2. Use of short-lived GFP for measuring 26S proteasome activity in living cells. In vivo 26S activity assays were performed in stable S2 cell lines constitutively expressing ubiquitin-GFP fusion proteins. (A) Diagram of the two destabilized GFP constructs and the stable M-GFP (6). The UFD construct, Ub<sup>G76V</sup>GFP, contains a ubiquitin sequence N-terminal of the GFP that is not cleaved by UPP but is further ubiquitinated and degraded by the 26S proteasome. The N-end rule substrate, Ub-R-GFP, is first cleaved by UPPs to generate a destabilizing Arg residue at the N terminus and then degraded by the proteasome. In the control Ub-GFP fusion, UPPs generate an N-terminal Met residue yielding a long-lived GFP. (B) Steady-state expression of Ub-GFP in stable *Drosophila* cell lines and effect of proteasome inhibition. Stable cell lines were treated for 3 h with 50 μM proteasome inhibitor MG132 and then collected along with untreated samples. The stabilities of the GFP constructs were analyzed by Western blotting with anti-GFP antibodies. Both short-lived GFP substrates are stabilized by proteasome inhibitor treatment. A nonspecific band detected by the anti-GFP antibodies is marked (\*).

metaphase blocks. All of this evidence taken together indicates that selective loss of DmS13 has profound effects on ubiquitin metabolism and cell cycle progression.

**In vivo *Drosophila* 26S proteasome assay.** To further explore the effects of DmS13 RNAi on proteasome activity and to avoid artifacts caused by purification of inherently unstable 26S complexes lacking individual subunits (12), we utilized an in vivo 26S activity assay. This reporter system was originally developed to monitor proteasome activity by using short-lived substrates produced in mammalian cell lines (6). Our approach involves stable *Drosophila* S2 cell lines constitutively expressing short-lived ubiquitin-GFP fusions (Fig. 2A) targeting two different ubiquitin-26S-dependent pathways (see the legend to Fig. 2). The Ub<sup>G76V</sup>GFP gene with an N-terminal ubiquitin is designed to function as a ubiquitin fusion degradation (UFD) substrate, while the Ub-R-GFP protein functions as an N-end

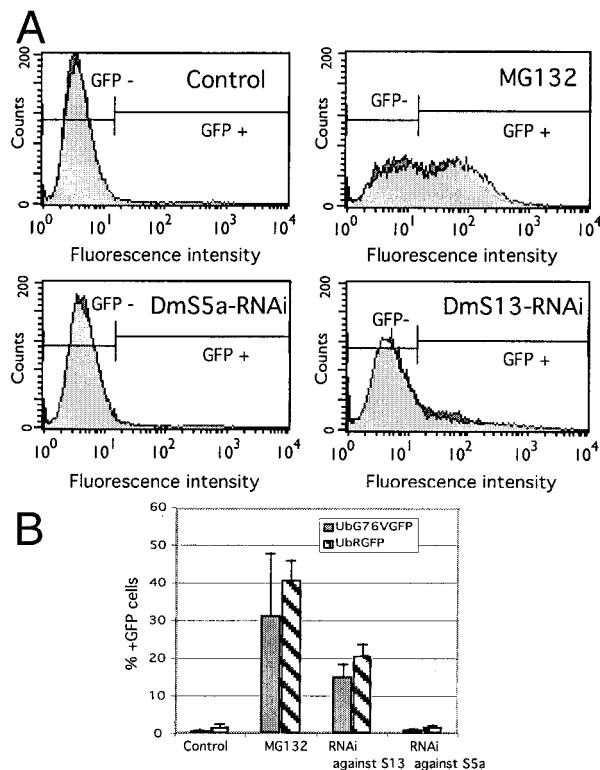


FIG. 3. Effects of DmS13 RNAi and DmS5a RNAi on proteasome-dependent GFP degradation. *Drosophila* S2 cell lines constitutively expressing short-lived proteasome substrates were treated with dsRNA against the DmS13 subunit or DmS5a. Four days posttreatment, flow cytometric analysis was performed to detect cells positive for either Ub<sup>G76V</sup>GFP (dark shading) or R-GFP (light shading). (A) Flow cytometric profiles of S2 cells that were either mock treated (control) or exposed to 50 μM MG132 (MG132) or to RNAi against DmS5a or DmS13, as indicated. The region defined as GFP- corresponds to the fluorescence intensity obtained for control cells lacking GFP. (B) Quantification of GFP stabilization after RNAi against either DmS13 or DmS5a or after treatment with the proteasome inhibitor MG132. The values were obtained from the treatments shown in panel A performed in triplicate. The error bars indicate standard deviations.

rule substrate. The two unstable substrates and a proteasome-resistant control fusion (Ub-M-GFP) were cloned into the constitutive *Drosophila* expression plasmid pAc5.1, and their steady-state expression was monitored by analysis of whole-cell extracts by immunoblotting them with anti-GFP antibodies. As expected, the Ub<sup>G76V</sup>GFP and Ub-R-GFP gene products were found to be short lived in the *Drosophila* cells, while the Ub-M-GFP control fusion was cleaved only by ubiquitin hydrolases (ubiquitin-processing proteases [UPPs]), yielding a stable M-GFP product (Fig. 2B).

To confirm that the short-lived GFP chimeras expressed in *Drosophila* S2 cells were ubiquitin-dependent 26S substrates targeted to distinct pathways, we monitored the stability of the fusions in the presence of the proteasome inhibitor MG132 (Fig. 2B) and tested the effect of a K48R mutation in the ubiquitin moiety of each substrate. The Western blot in Fig. 2B shows that in the presence of MG132, both the UFD and the N-end rule substrates were no longer degraded by the proteasome. The band detected with anti-GFP antibodies matched

the expected molecular weight for the intact Ub<sup>G76V</sup>GFP fusion, while Ub-R-GFP was still processed by ubiquitin hydrolases to a GFP molecule containing an Arg N terminus. As expected from previous characterizations of the two pathways (23), the UFD substrate Ub<sup>G76V</sup>GFP was stabilized by the K48R mutation, while the N-end rule substrate, Ub-R-GFP, was unaffected and maintained a short half-life (data not shown). In both cases, the stabilization of both substrates detected by Western blotting correlated with increased GFP fluorescence intensity in flow cytometric analysis. These results show that Ub<sup>G76V</sup>GFP and Ub-R-GFP are true 26S substrates in S2 cells. Their degradation reflects 26S proteasome activity, and fluorescent signals resulting from their stabilization directly correlated with fusion protein levels within the cell.

RNAi-mediated inhibition of DmS13 increased fluorescence, indicating GFP accumulation in S2 cells constitutively expressing either of the 26S proteasome substrates (Fig. 3A). The overall substrate levels were ~4-fold higher than those of controls or DmS5a knockout cells (Fig. 3B). This is a relevant difference, considering that RNAi against DmS5a and DmS13 were equally effective in knocking down their respective target proteins. A significantly higher fraction of cells exhibited substrate stabilization with MG132, yet the cells that did show GFP stabilization from the DmS13 RNAi treatment had levels of GFP fluorescence equal to or greater than those with the MG132 treatment. This effect may be explained by the lower efficiency of RNAi compared to chemical proteasome inhibition with MG132 (see Discussion). Thus, a smaller fraction of the RNAi-treated cells undergo complete knockout of the DmS13 subunit, while the remaining cells contain residual 26S activity. In fact, dsRNA directed against the 20S catalytic subunit Prosβ2 was also less efficient than MG132 and yielded results similar to those of DmS13 RNAi (data not shown). Finally, fluorescence microscopy examination showed that for both substrates, DmS13 knockdown and MG132 treatment led to approximately equivalent accumulations of GFP in both the nuclei and cytoplasm of the *Drosophila* cells, indicating that proteasome activity was affected in all cellular compartments (data not shown).

**Loss of the S13 subunit and 26S proteasome integrity.** As shown above, the loss of the DmS13 subunit led to cell cycle arrest and inhibition of ubiquitin-dependent degradation of short-lived GFPs. The S13 subunit contains a number of conserved domains that may serve critical functions, and the specific loss of these activities could be the cause of the observed defects. Alternatively, the results could also be explained by an overall instability or lack of assembly of the 26S proteasome after removal of DmS13 from the complex. To address these points, nondenaturing gel electrophoresis was carried out to compare the amounts of 26S proteasome present in control and RNAi-treated cell extracts. Intact 26S and 20S proteasomes were identified using both in-gel peptidase assays and Western blots, while RNAi-mediated inhibition of DmS13 was again confirmed by Western blot analysis performed on cell extracts fractionated on a SDS gel. As a reference for the changes in migration pattern involved in 26S disassembly and to estimate the total amount of 20S present, we used a control lysate depleted of ATP. In this sample, 26S dissociated into its components, resulting in the disappearance of the 26S band and the accumulation of uncapped 20S proteasomes (Fig. 4A,

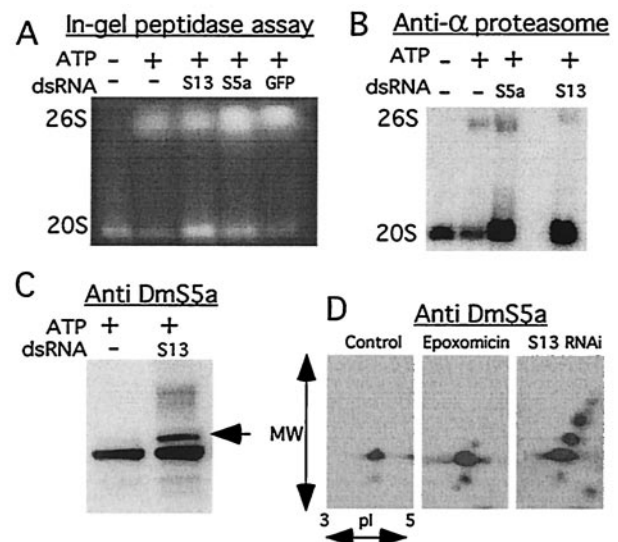


FIG. 4. Effects of DmS13 RNAi on proteasome activity and subunit expression. (A) RNAi-treated and control extracts were prepared in the absence (–) or presence (+) of 4 mM ATP. In ATP– samples, endogenous ATP was depleted by apyrase treatment. Equivalent amounts of total protein were separated by native gel electrophoresis, and in-gel peptidase assays were carried out by overlaying with the fluorogenic proteasome substrate LLVY-MCA, followed by exposure to UV light. Elevated 20S activity becomes apparent after DmS13 or DmS5a RNAi treatment. The total amount of 20S proteasome in untreated cells was estimated by the fluorescence in the 20S band of the apyrase-treated control (left lane). (B) Extracts from control cells with and without ATP (two left lanes) and cells exposed to DmS5a RNAi (middle lane) or DmS13 RNAi (right lane) were separated by native gel electrophoresis, transferred to membranes, and probed with anti- $\alpha$ -proteasome antibodies. (C) Extracts from control (–) and DmS13 RNAi-treated cells were separated by SDS-PAGE and immunoblotted with anti-S5a antibodies. Loss of S13 leads to the up-regulation of S5a and to the appearance of a slower-migrating band (arrow). (D) Two-dimensional PAGE of DmS13 RNAi-treated extracts immunoblotted with anti-S5a antibodies (right). Extracts from control or epoxomicin-treated cells are shown in the left and middle panels, respectively.

left lane). As shown in Fig. 4, there was no observable difference in the levels or migration behavior of the 26S proteasome in DmS13 RNAi-treated cells compared to control cells.

However, loss of DmS13 or DmS5a led to an ~2-fold increase of 20S proteasome levels as determined by in-gel activity assay (Fig. 4A and 5C). Western blot quantification of the 20S levels carried out on apyrase-treated samples transferred from nondenaturing gels confirmed that approximately twice as many active 20S proteasomes were assembled upon DmS13 depletion compared to controls (Fig. 4B). A similar increase in 20S proteasome levels was also observed for DmS5a-depleted cells (Fig. 4B, middle lane). This was not a nonspecific response to dsRNA or to compromised cell viability. In fact, RNAi treatment targeting GFP left proteasome levels unaffected (Fig. 4A). On the other hand, DmS5a-depleted cells showed only modest defects in cell cycle progression or viability but also led to increased amounts of cellular 20S proteasomes. Notably, DmS13 and DmS5a RNAi-treated cells also contained higher levels of DmS5a and DmS13, respectively (Fig. 1A and 4D), indicating that expression of 19S compo-

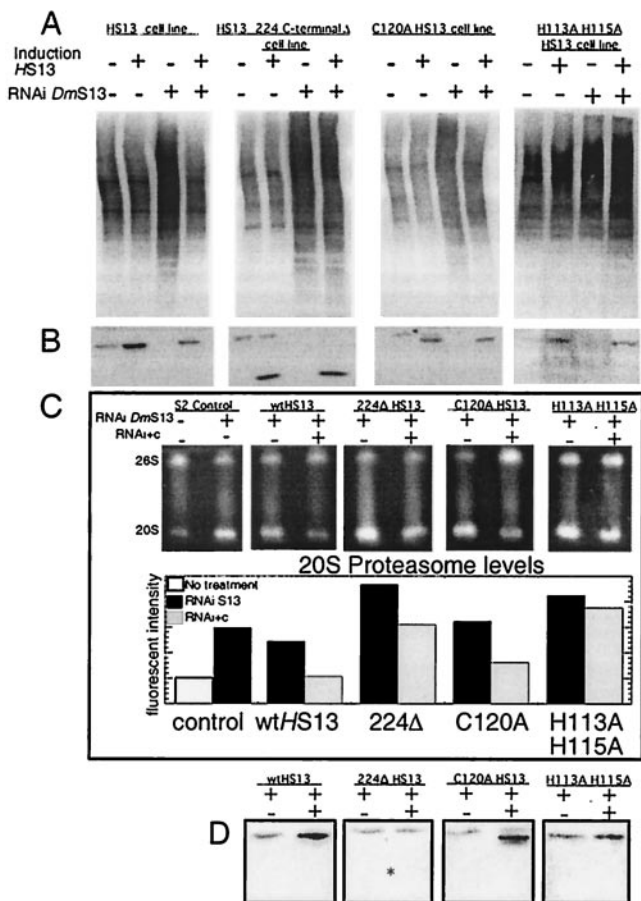


FIG. 5. HS13 is a functional homolog of *Drosophila* S13. Four distinct stable S2 cell lines containing inducible forms of the wild-type HS13, HS13Δ224, HS13C120A, or HS13 H113A-H115A were subjected to RNAi to eliminate the *Drosophila* S13 subunit. Immunoblots were carried out using anti-ubiquitin chain antibodies or anti-S13 antibodies. (A) Top section of the Western blot probed with anti-ubiquitin antibodies to compare ubiquitin conjugate pool levels. The HS13C120A mutant can partially restore ubiquitin conjugate pool levels. +, present; -, absent. (B) Western blot probed with anti-S13 antibodies showing levels of endogenous DmS13 and of induced HS13 in RNAi+c experiments. To confirm that equivalent amounts of total protein were loaded, the blot shown in panel A was stained for total protein after Western blot development (not shown). (C) Equivalent amounts of total protein were separated by native gel electrophoresis, and in-gel peptidase assays were carried out by overlaying with the fluorogenic-proteasome substrate LLVY-MCA, followed by exposure to UV light. The rescue of elevated 20S activity after RNAi treatment by the expression of HS13 wild type or mutants was estimated by the 20S fluorescence intensities, and a digitized image was quantified using Image Gauge analysis software (bottom). (D) From in-gel peptidase assays, the 26S bands were cut out and then separated by SDS-PAGE, followed by immunoblotting with anti-S13 antibodies. The expected migration position for HS13Δ224 is marked (\*).

nents are influenced by deletion of individual subunits. In addition to these changes in subunit expression, which confirm published reports (56), we observed an apparent modification of the DmS5a subunit following DmS13 knockdown (Fig. 4C). Modified DmS5a, which was not observed in previous studies, was identified as a slower-migrating band ~8 to 9 kDa above the typical S5a band in untreated extracts and could be re-

solved into two or three species by two-dimensional PAGE (Fig. 4D, right). The exact nature of this modification is unknown, although we favor the hypothesis of conjugation with ubiquitin moieties (see Discussion).

**DmS13 RNAi+c.** To address the effects of S13 mutations and the functions of conserved domains of the S13 subunit, we combined DmS13 RNAi with complementation involving HS13 genes under the control of the CuSO<sub>4</sub>-inducible metallothionein promoter. To this end, we generated four distinct recombinant S2 cell lines stably transfected with either wild-type HS13 or three mutant genes previously shown to have profound effects on proteasome function and cell metabolism (see Discussion). Mutant HS13C120A contained a single-site substitution within the conserved MPN/JAMM domain (see Discussion). A double mutant HS13 (H113A-H115A) contained mutations in the proposed metalloisopeptidase active site of S13 (numbering based on the HS13 sequence) (51, 58). The C-terminal deletion mutant HS13Δ224 was truncated at residue C224. First, a range of copper sulfate concentrations was tested to determine an optimal induction level for the human proteasome subunit. In the absence of CuSO<sub>4</sub>, no apparent expression was detectable, while at 300 μM CuSO<sub>4</sub>, the cells expressed significant and roughly equivalent amounts of wild-type or mutant HS13s (Fig. 5B). At these concentrations, no detectable effects on ubiquitin conjugate levels was observed in three of the stable cell lines (Fig. 5A), as determined by anti-ubiquitin immunoblotting. However, for a fourth stable cell line containing the H113A-H115A double mutation, increased levels of ubiquitin conjugates were observed after induction with CuSO<sub>4</sub>.

To determine whether the HS13 subunit could functionally substitute for DmS13 in depleted cells, we examined ubiquitin metabolism in cells undergoing RNAi or RNAi+c treatment. Equivalent amounts of total protein were fractionated by SDS-PAGE and probed with an anti-ubiquitin antibody (Fig. 5A). As expected, all cell lines exhibited increased ubiquitin conjugate levels after RNAi treatment against DmS13. Upon expression of wild-type HS13, the ubiquitin conjugate pool returned to the levels observed in untreated control cells, while both the C-terminal truncation HS13Δ224 and HS13 (H113A-H115A) were unable to restore normal ubiquitin conjugate metabolism. The RNAi+c-treated cells expressing HS13C120A exhibited an intermediate level of ubiquitin chains, indicating partial recovery of conjugate processing. As mentioned previously, RNAi knockdown of DmS13 resulted in the formation of a modified form of DmS5a. RNAi+c-treated cells with either the wild-type HS13 or the C120A mutant exhibited a single band corresponding to the unmodified DmS5a, but the C-terminal truncation HS13Δ224- and the H113A-H115A-treated cells still contained the modified form of S5a (data not shown).

To determine whether HS13 incorporation into viable *Drosophila* 26S proteasomes might in part explain these differences, RNAi+c cell extracts were fractionated by native PAGE. Following detection by in-gel activity assay (Fig. 5C), the 26S bands were excised and run on a denaturing SDS gel, and the HS13 subunits were detected by immunoblotting with anti-S13 antibodies. The induction of 20S proteasome levels was apparent when DmS13 was knocked down (Fig. 5C, left). RNAi+c with wild-type or C120A HS13 led to a return to

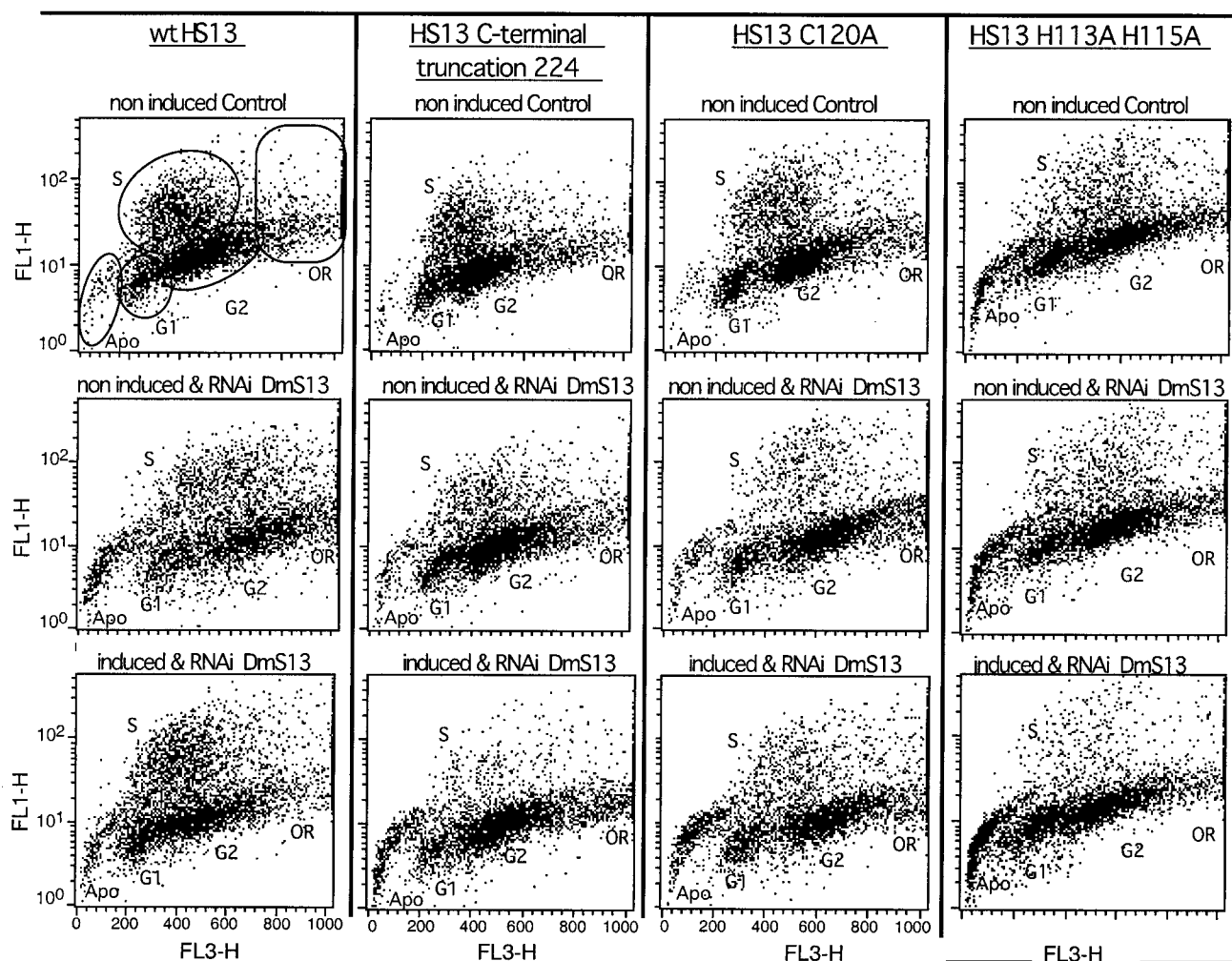


FIG. 6. Wild-type (wt) HS13 restores cell cycle progression in *Drosophila* S13-depleted cells. Stable *Drosophila* S2 cell lines containing inducible forms of the HS13 gene were induced with copper sulfate and also treated with dsRNA to remove the *Drosophila* host subunit. The cells were labeled with BrdU to measure newly synthesized DNA (y axis) and stained with 7-AAD (x axis) for total cellular DNA. The specific cell cycle regions are marked in the first control sample (OR, overreplicating cells). The sub- $G_0$  fraction was confirmed to represent apoptotic cells by comparison with apoptotic S2 cells (Apo) induced by staurosporine. Top row, untreated cells; middle row, cells exposed to DmS13 RNAi only; bottom row, cells exposed to DmS13 RNAi and expressing HS13, HS13 $\Delta$ 224, HS13C120A, or HS13 H113A-H115A, as indicated.

control proteasome levels, while expression of HS13 $\Delta$ 224 or H113A-H115A did not prevent the up-regulation of the proteasome levels (Fig. 5C). Wild-type HS13, C120A HS13, and H113-H115A were apparently incorporated at significant levels into the *Drosophila* 26S proteasome, while HS13 $\Delta$ 224 exhibited barely detectable levels of incorporation (Fig. 5D). Surprisingly, a larger amount of residual DmS13 was observed from the excised 26S bands relative to the overall cellular DmS13 levels after RNAi-mediated knockdown.

To further test whether the rescue of ubiquitin turnover may parallel correction of metabolic defects, we analyzed cycle progression in RNAi+c-treated cells. To this end, we performed FACS analysis of all four stable recombinant S2 cell lines. As illustrated by the top four scatter plots in Fig. 6, three of the stable transfectants exhibited very similar cell cycle patterns in the absence of RNAi or RNAi+c. However, a distinct difference was observed with the proposed active-site mutant

H113A-H115A, which had increased levels of apoptotic cells before and during induction. The higher apoptotic levels of the H113A-H115A stable cell line was confirmed by a second apoptotic flow cytometry assay (41) (data not shown). In agreement with the previous experiments, in the absence of HS13 complementation, the cells showed increased apoptosis after DmS13 RNAi (Fig. 6, middle). An overall increase of the total DNA content, indicative of DNA overreplication, was also observed in these samples. This is illustrated by the strong shift to the right on the x axis in the middle scatter plots of Fig. 6 and by the diagrams presented in Fig. 7. Induction of the wild-type HS13 normalized the cell cycle progression and decreased the overall DNA content significantly. The number of apoptotic cells was also found to drop substantially upon HS13 expression, almost reaching control levels (Fig. 6 and 7). The mutant forms of HS13 were unable to rescue the defects in RNAi-treated cell lines (Fig. 6 and 7). While HS12 $\Delta$ 224 had no

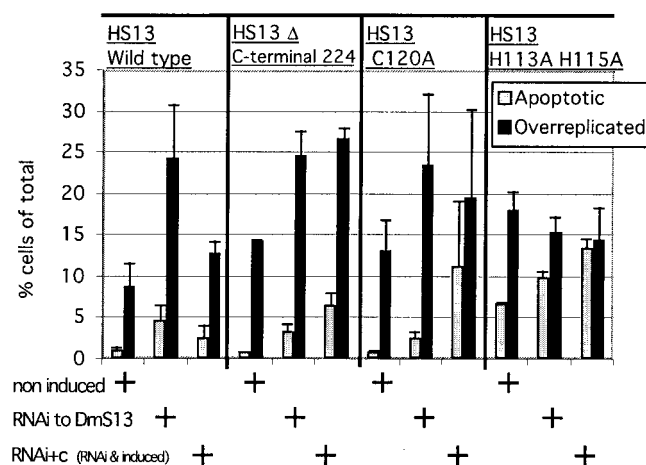


FIG. 7. Mutant forms of HS13 do not rescue DmS13-depleted cells from apoptosis or DNA overreplication. Stable *Drosophila* S2 cells containing inducible wild-type or mutant forms of HS13 were treated with dsRNA to remove endogenous DmS13 and exposed to copper sulfate to induce HS13 expression. Apoptotic-cell subpopulations and cells undergoing DNA overreplication were quantified by flow cytometric analysis using constant gating parameters. The graph shows averages (plus standard deviations) from experiments carried out in triplicate.

detectable effects, induction of HS13C120A surprisingly resulted in even higher levels of apoptosis and a continued overreplication of total DNA. As expected for a potential isopeptidase active-site mutant, the H113-H115A cell line was unable to rescue and showed the highest apoptotic levels. The levels of DNA overreplication were modestly higher for the H113-H115A cell line than for control cells and did not change significantly during RNAi or RNAi+c treatment.

## DISCUSSION

The 19S particle is a complex essential for the proteasome-dependent degradation of proteins. 19S binds to either end of the 20S proteasome catalytic core and is critically involved in the processing of conjugates prior to their degradation. Processing includes binding of ubiquitin chains, deubiquitinylation, substrate unfolding, and translocation into the catalytic chamber. Little is known about the specific functions of the non-ATPase subunits of the 19S lid, although deubiquitinylation activities necessary to “unchain the substrate” for further unfolding and translocation have been traced to this subcomplex (55).

Lid subunits show extensive homology with other complexes, such as the COP9-signalosome or eIF3. The closest relatives are the lid subunit, S13, and the COP9-signalosome component Csn5 (JAB1), which, besides extensive overall homology, also exhibit marked conservation of putative catalytic domains. In fact, yeast S13 was recently shown to contain a metalloisopeptidase activity that couples substrate deubiquitinylation with ATP-dependent degradation (51, 58), while Csn5 was identified as a related metalloisopeptidase that removes the ubiquitin-like Nedd8 from proteins (5). Notably, of all signalosome subunits, only the S13 homolog, Csn5, is present in the budding yeast *Saccharomyces cerevisiae* (42), further suggesting

a basic function for this class of subunits. While yeast S13 is well characterized, little is known about the physiological role of the metazoan homolog. To study the functions of DmS13 and HS13, we combined DmS13 RNAi with complementation using HS13. This approach, which we called RNAi+c, is made possible by the fact that HS13 and DmS13 show <80% sequence identity and are thus not expected to share any dsRNA interference (2). With RNAi+c, we addressed two main points. The first was the ability of HS13 to act as a functional homolog of DmS13. The second was the effects of three HS13 mutations: a double mutation of two proposed isopeptidase active-site histidines, a single-residue substitution in a putative domain near the active site, and, finally, a C-terminal truncation. Compared to an analogous approach involving inducible RNAi of *Trypanosoma brucei* subunits in cells constitutively expressing yeast subunits (29), our experimental setup involves S2 cells stably transfected with CuSO<sub>4</sub>-inducible forms of HS13s.

Consistent with previous observations made in yeast, DmS13 depletion leads to apoptosis, DNA overreplication, and cell cycle block (33, 36). In addition, we found significant accumulation of cells arresting at metaphase. A similar alteration was reported for yeast mutants containing a defective S13 (33), while RNAi-mediated inhibition of other 19S subunits in *Drosophila* cells caused apoptosis and impaired cell cycle progression without specific cell cycle blocks (56). The mechanisms involved in metaphase arrest are unknown. However, the transition to anaphase involves a number of important proteolytic events that require ubiquitin-dependent 26S proteasome activity (39) and contributions from the N-end rule pathway (34), both of which may be impaired in DmS13-depleted cells. In this regard, we found that DmS13 loss in fact induces a substantial accumulation of ubiquitin conjugates, indicating a profound impact on the processing of ubiquitinated substrates. The magnitude of this defect is comparable to complete disruption of proteasome activity induced by RNAi targeting the essential catalytic 20S core subunit Prosβ2. This was further confirmed by *in vivo* measurements of 26S activity using short-lived fluorescent proteasome substrates (Ub-GFPs). Proteasome inhibition and consequent stabilization of the substrates results in increased fluorescence signals detectable by flow cytometric analysis (6). With this approach, we detected biologically relevant levels of proteasome inhibition while avoiding known artifacts caused by the purification of proteasomes from cells depleted of individual subunits (13). Furthermore, we were able to measure 26S activity in individual cells by flow cytometry rather than determining the average activity in extracts of a cell population exposed to RNAi. This is an important advantage if depletion by RNAi fluctuates in efficiency from cell to cell.

While the GFP substrates were basically undetectable in untreated cells, RNAi-mediated inhibition of DmS13 led to stabilization of the *in vivo* 26S proteasome substrates. Both the N-end rule and UFD substrates (Ub-R-GFP and Ub<sup>G76V</sup>GFP, respectively) were stabilized when DmS13 was depleted from S2 cells. However, the fraction of cells exhibiting GFP stabilization was significantly lower for DmS13 RNAi than for MG132 treatment. We favor an explanation that takes into account two important factors. The first is the likely lower efficiency of dsRNA interference compared to chemical inhi-

bition. Second is the probable loss of DmS13-depleted cells during RNAi treatment prior to FACS analysis: 3 to 4 days of RNAi compared to a 3-h exposure to MG132. The toxic effect of DmS13 depletion may in fact selectively subtract from FACS analysis those cells that completely eliminate DmS13 for an extended period of time. In support of this explanation, we determined that RNAi-mediated DmS13 and Pros $\beta$ 2 knock-down yielded similar numbers of fluorescent cells. In both cases, positive cells contained equal or even higher GFP levels than for MG132 treatment. These data taken together indicate that the impact of DmS13 knockdown on the ubiquitin-proteasome pathway is comparable to complete loss of proteasome activity.

However, DmS13 RNAi did not compromise the catalytic activity of the 20S core particle. On the contrary, 20S proteasome levels and activity in depleted cells were increased compared to controls (see below). In line with published data on yeast S13, DmS13 thus appears to be involved in rate-limiting steps preceding catalytic attack, namely, substrate deubiquitinylation (31, 51). Unlike the ubiquitin carboxy-terminal hydrolase of the *Drosophila* proteasome p37A (UCH37), which can be eliminated without deleterious effects (56), the deubiquitinating activity of DmS13 appears to be essential for 26S function. Similar conclusions were drawn from analysis of budding yeast cells harboring the Rpn11 mutant. 26S dysfunction was explained with specific loss of lid subunits from the proteasomes of yeast encoding mutant Rpn11, as demonstrated by aberrant 26S migration patterns on nondenaturing gels (51). Similar mechanisms were suggested for the effects of subunit depletion in *Drosophila* and yeast (40, 56). Surprisingly, repeated analysis did not reveal obvious differences between the 26S proteasomes from DmS13-depleted samples and control extracts. We conclude that a significant amount of 26S proteasome is present in the RNAi-treated S2 cells and suggest that the DmS13 contribution to 26S activity is mainly nonstructural.

These results also suggest that the phenotypes observed after DmS13 depletion essentially result from the loss of its catalytic functions, in line with its classification into the JAMM/MPN<sup>+</sup> family (31, 51). In this regard, we found that wild-type HS13, which contains the strictly conserved JAMM/MPN<sup>+</sup> motif, fully rescues DmS13 RNAi-dependent phenotypes. HS13 normalized ubiquitin conjugates, 20S proteasome levels, and cell proliferation. In agreement with recent yeast studies, histidine mutations in the proposed isopeptidase active site prevented the rescue of ubiquitin conjugate pool levels. On the other hand, DmS13-depleted cells expressing HS13C120A exhibited slightly elevated levels of ubiquitin conjugates compared to controls and contained normal levels of 20S proteasomes, indicating that HS13C120A rescued, to a great extent, proteasome functions. Thus, a highly conserved cysteine residue characteristic of deubiquitinating enzymes (C120 in HS13), but separate from the recently proposed isopeptidase JAMM motif, is not absolutely essential for S13 activity. This cysteine residue is conserved in all known S13 sequences with the exception of the S13 subunit of *Giardia*. The residual conjugates may reflect a limited functional defect in 26S harboring the mutant subunit and affecting a nonspecific set of proteins. However, this is hardly compatible with the massive defects still present in cells complemented with HS13C120A. These cells still exhibited the abnormal DNA duplication and high

levels of apoptosis observed in noncomplemented DmS13-depleted cells. This suggests a specific role for C120 in the regulation of key cell proliferation and/or proapoptotic factors. The stabilized conjugates may thus represent a discrete subpopulation of ubiquitinated regulators that require C120 for their degradation. Such a possibility has been suggested for defects observed after Rpn6 depletion in yeast (40). Alternatively, this specific set of proteins could require C120 for reactions not associated with proteasome-dependent proteolysis, analogous to similar functions suggested for 19S (7, 10, 14, 38). Whether these putative S13 functions or activities are strictly related to DNA metabolism is unknown. However, S13 has been directly linked to resistance to UV light and to chemical DNA-damaging agents and to the regulation of chromatin structure (1, 43, 44, 48).

Our results suggest that S13 requires incorporation into 19S. No enzymatic activity was found with purified recombinant human (C. Realini, unpublished observation) or yeast homologs of DmS13 (33). In addition, the C-terminally truncated HS13 $\Delta$ 224, with an intact JAMM/MPN<sup>+</sup> catalytic motif but unable to assemble with 19S, could not rescue any RNAi-DmS13 depletion phenotypes. For three of the four stable cell lines, detectable phenotypes from overexpression of wild-type or mutant HS13s were observed only in S2 cells depleted of the endogenous subunits. Surprisingly, the active-site mutant H113A-H115A showed both increased ubiquitin conjugate pools and a higher proportion of apoptotic cells before RNAi-mediated inhibition of DmS13. A possible explanation for these results is that even quite low levels of HS13 H113A-H115A are highly toxic for *Drosophila* S2 cells. In fact, the generation of a stable isopeptidase mutant cell line was obtainable only after a number of unsuccessful attempts.

As mentioned above, cells depleted of DmS13 or DmS5a exhibited higher levels of uncapped 20S proteasome. This up-regulation was first detected as increased 20S activity by fluorogenic overlay assay of native gels. These results, further confirmed by Western blot analysis using anti-20S antibodies, indicate that larger amounts of fully active complexes were assembled when the levels of DmS13 declined. RNAi-mediated depletion of DmS13 did not affect the levels of the proteasome activator REG $\gamma$  but did induce up-regulation of DmS5a. These results are in agreement with recent work showing that the removal of one proteasome gene could specifically increase the levels of other 20S and 19S subunits (56). Recently, concerted up-regulation of mammalian 26S proteasome subunit mRNAs has been observed when cells are treated with a proteasome inhibitor (32).

The regulatory mechanisms involved in the 20S up-regulation are unclear. In this study, proteasomes returned as expected to control levels in cells complemented with wild-type HS13, but also in cells expressing HS13C120A that still exhibited significant metabolic defects. Thus, proteasome up-regulation could be a direct and reversible response to subtle changes in 26S structure and/or function resulting from subunit loss rather than to impaired metabolism. Proteasome dysfunction may stabilize a yet-undiscovered putative *Drosophila* homolog of yeast Rpn4, a transcriptional activator of proteasome genes and short-lived proteasome substrate (57).

As discussed above, the loss of DmS5a resulted in a moderate accumulation of ubiquitin conjugates without detectable

metabolic defects. Recent work has demonstrated that the loss of DmS5a causes a larval-pupal lethality and a large increase in 26S proteasome levels for *Drosophila* (45). However, the loss of S5a did not stabilize either the N-end rule or the UFD short-lived GFP. In *S.cerevisiae*, the loss of S5a or Rpn10, or deletions in the N terminus of Rpn11, results in stabilization of the UFD pathway substrate, Ub-Pro- $\beta$  galactosidase (9). Although we measured proteasome activity in individual cells, we did not detect any accumulation of the UFD substrate upon S5a depletion, suggesting that DmS5a may not play an essential role for UFD proteasome degradation in metazoan cells.

In S2 cells, DmS5a is generally detected as a single species (this work and reference 21). Following DmS13 depletion, however, we detected a slower-migrating form of DmS5a that could be resolved by two-dimensional gels into at least two or three species. Since sequence considerations do not support the existence of an unprocessed DmS5a precursor, we propose that these forms represent a newly discovered posttranslational modification, possibly ubiquitinylation. In fact, the migration of modified DmS5a on two-dimensional gels is compatible to an addition of one to three ubiquitin moieties, which were detected in preliminary immunoblots using anti-ubiquitin antibodies. Notably, an analogous modification was described for Eps15 (24), which, like S5a, belongs to a large class of proteins containing polyubiquitin-binding UIMs (ubiquitin-interacting motifs) (20). We are identifying the nature of the modification and its effects on S5a and the 19S regulatory complex.

In conclusion, we have shown here that S13 is an essential and evolutionarily conserved subunit of the metazoan 26S proteasome. Consistent with previous observations with other 19S subunits, DmS13 deletion yields pleiotropic phenotypes that involve the ubiquitin-proteasome system. These effects are not mediated by direct inhibition of the 20S proteasome catalytic sites. Rather, DmS13 is responsible for a rate-limiting event prior to catalytic attack, in line with the proposed role as a zinc-binding deubiquitinating enzyme. We suggest that S13 also possesses functions that regulate progression through the cell cycle and that it requires C120. In general, RNAi+c should be a useful technique to study metazoan proteins. Our RNAi+c approach, combined with in vivo proteasome activity assays, provides the basis for a wider set of complementation studies involving additional mutants aimed at mapping key domains within S13 and other proteasome subunits.

#### ACKNOWLEDGMENTS

C.A.R. and P.Y. are co-senior authors of this paper.

We thank Nico Dantuma and Maria Masucci for the original short-lived GFP vectors, Chris Norbury for discussions on the S13 subunit, Ann-Christine Östlund-Farranz for tubulin antibody, Uli Theopold for *Drosophila* hemomucin antibody, Andor Udvardy from the Biological Research Center of the Hungarian Academy of Sciences for the generous gift of a *Drosophila* S5a (p54) cDNA clone, Petra Björk for help with the fluorescence microscopy, and Alf Grandien for FACS analysis, suggestions, and protocols.

This work was supported by grants from the Swedish Research Council and the Carl Tryggers Stiftelse.

#### REFERENCES

- Arioka, M., M. Kouhashi, K. Yoda, A. Takatsuki, M. Yamasaki, and K. Kitamoto. 1998. Multidrug resistance phenotype conferred by overexpressing *bfr2+/pad1+/sks1+* or *pap1+* genes and mediated by *bfr1+* gene product, a structural and functional homologue of P-glycoprotein in *Schizosaccharomyces pombe*. *Biosci. Biotechnol. Biochem.* **62**:390–392.
- Bosher, J. M., and M. Labouesse. 2000. RNA interference: genetic wand and genetic watchdog. *Nat. Cell Biol.* **2**:E31–E36.
- Braun, B. C., M. Glickman, R. Kraft, B. Dahlmann, P. M. Kloetzel, D. Finley, and M. Schmidt. 1999. The base of the proteasome regulatory particle exhibits chaperone-like activity. *Nat. Cell Biol.* **1**:221–226.
- Clemens, J. C., C. A. Worby, N. Simonson-Leff, M. Muda, T. Machama, B. A. Hemmings, and J. E. Dixon. 2000. Use of double-stranded RNA interference in *Drosophila* cell lines to dissect signal transduction pathways. *Proc. Natl. Acad. Sci. USA* **97**:6499–6503.
- Cope, G. A., G. S. Suh, L. Aravind, S. E. Schwarz, S. L. Zipursky, E. V. Koonin, and R. J. Deshaies. 2002. Role of predicted metalloprotease motif of Jab1/Csn5 in cleavage of Nedd8 from Cul1. *Science* **298**:608–611.
- Dantuma, N. P., K. Lindsten, R. Glas, M. Jellne, and M. G. Masucci. 2000. Short-lived green fluorescent proteins for quantifying ubiquitin/proteasome-dependent proteolysis in living cells. *Nat. Biotechnol.* **18**:538–543.
- Ferdous, A., F. Gonzalez, L. Sun, T. Kodadek, and S. A. Johnston. 2001. The 19S regulatory particle of the proteasome is required for efficient transcription elongation by RNA polymerase II. *Mol. Cell* **7**:981–991.
- Ferrell, K., C. R. Wilkinson, W. Dubiel, and C. Gordon. 2000. Regulatory subunit interactions of the 26S proteasome, a complex problem. *Trends Biochem. Sci.* **25**:83–88.
- Fu, H., N. Reis, Y. Lee, M. H. Glickman, and R. D. Vierstra. 2001. Subunit interaction maps for the regulatory particle of the 26S proteasome and the COP9 signalosome. *EMBO J.* **20**:7096–7107.
- Gillette, T. G., W. Huang, S. J. Russell, S. H. Reed, S. A. Johnston, and E. C. Friedberg. 2001. The 19S complex of the proteasome regulates nucleotide excision repair in yeast. *Genes Dev.* **15**:1528–1539.
- Glickman, M. H., and V. Maytal. 2002. Regulating the 26S proteasome. *Curr. Top. Microbiol. Immunol.* **268**:43–72.
- Glickman, M. H., D. M. Rubin, O. Cox, I. Wefes, G. Pfeifer, Z. Cjeka, W. Baumeister, V. A. Fried, and D. Finley. 1998. A subcomplex of the proteasome regulatory particle required for ubiquitin-conjugate degradation and related to the COP9-signalosome and eIF3. *Cell* **94**:615–623.
- Glickman, M. H., D. M. Rubin, H. Fu, C. N. Larsen, O. Cox, I. Wefes, G. Pfeifer, Z. Cjeka, R. Vierstra, W. Baumeister, V. Fried, and D. Finley. 1999. Functional analysis of the proteasome regulatory particle. *Mol. Biol. Rep.* **26**:21–28.
- Gonzalez, F., A. Delahodde, T. Kodadek, and S. A. Johnston. 2002. Recruitment of a 19S proteasome subcomplex to an activated promoter. *Science* **296**:548–550.
- Gorbea, C., D. Taillandier, and M. Rechsteiner. 1999. Assembly of the regulatory complex of the 26S proteasome. *Mol. Biol. Rep.* **26**:15–19.
- Groll, M., L. Ditzel, J. Lowe, D. Stock, M. Bochtler, H. D. Bartunik, and R. Huber. 1997. Structure of 20S proteasome from yeast at 2.4 Å resolution. *Nature* **386**:463–471.
- Groll, M., Y. Koguchi, R. Huber, and J. Kohno. 2001. Crystal structure of the 20S proteasome: TMC-95A complex: a non-covalent proteasome inhibitor. *J. Mol. Biol.* **311**:543–548.
- Haraeska, L., and A. Udvardy. 1997. Mapping the ubiquitin-binding domains in the p54 regulatory complex subunit of the *Drosophila* 26S protease. *FEBS Lett.* **412**:331–336.
- Hershko, A., E. Leshinsky, D. Ganoth, and H. Heller. 1984. ATP-dependent degradation of ubiquitin-protein conjugates. *Proc. Natl. Acad. Sci. USA* **81**:1619–1623.
- Hofmann, K., and L. Falquet. 2001. A ubiquitin-interacting motif conserved in components of the proteasomal and lysosomal protein degradation systems. *Trends Biochem. Sci.* **26**:347–350.
- Holz, H., B. Kapelari, J. Kellermann, E. Seemuller, M. Sumegi, A. Udvardy, O. Medalia, J. Sperling, S. A. Muller, A. Engel, and W. Baumeister. 2000. The regulatory complex of *Drosophila melanogaster* 26S proteasomes. Subunit composition and localization of a deubiquitinating enzyme. *J. Cell Biol.* **150**:119–130.
- Hough, R., G. Pratt, and M. Rechsteiner. 1986. Ubiquitin-lysozyme conjugates. Identification and characterization of an ATP-dependent protease from rabbit reticulocyte lysates. *J. Biol. Chem.* **261**:2400–2408.
- Johnson, E. S., P. C. Ma, I. M. Ota, and A. Varshavsky. 1995. A proteolytic pathway that recognizes ubiquitin as a degradation signal. *J. Biol. Chem.* **270**:17442–17456.
- Klapisz, E., I. Sorokina, S. Lemeur, M. Pijnenburg, A. J. Vekleij, and P. M. van Bergen en Henegouwen. 2002. A ubiquitin-interacting motif (UIM) is essential for Eps15 and Eps15R ubiquitination. *J. Biol. Chem.* **277**:30746–30753.
- Lam, Y. A., T. G. Lawson, M. Velayutham, J. L. Zweier, and C. M. Pickart. 2002. A proteasomal ATPase subunit recognizes the polyubiquitin degradation signal. *Nature* **416**:763–767.
- Lam, Y. A., W. Xu, G. N. DeMartino, and R. E. Cohen. 1997. Editing of ubiquitin conjugates by an isopeptidase in the 26S proteasome. *Nature* **385**:737–740.
- Layfield, R., K. Franklin, M. Landon, G. Walker, P. Wang, R. Ramage, A. Brown, S. Love, K. Urquhart, T. Muir, R. Baker, and R. J. Mayer. 1999. Chemically synthesized ubiquitin extension proteins detect distinct catalytic capacities of deubiquitinating enzymes. *Anal. Biochem.* **274**:40–49.

28. Leggett, D. S., J. Hanna, A. Borodovsky, B. Crosas, M. Schmidt, R. T. Baker, T. Walz, H. Ploegh, and D. Finley. 2002. Multiple associated proteins regulate proteasome structure and function. *Mol. Cell* **10**:495–507.
29. Li, Z., and C. C. Wang. 2002. Functional characterization of the 11 non-ATPase subunit proteins in the trypanosome 19S proteasomal regulatory complex. *J. Biol. Chem.* **277**:42686–42693.
30. Lowe, J., D. Stock, B. Jap, P. Zwickl, W. Baumeister, and R. Huber. 1995. Crystal structure of the 20S proteasome from the archaeon *T. acidophilum* at 3.4 Å resolution. *Science* **268**:533–539.
31. Maytal-Kivity, V., N. Reis, K. Hofmann, and M. H. Glickman. 2002. MPN+, a putative catalytic motif found in a subset of MPN domain proteins from eukaryotes and prokaryotes, is critical for Rpn11 function. *BMC Biochem.* **3**:28.
32. Meiners, S., D. Heyken, A. Weller, A. Ludwig, K. Stangl, P. M. Kloetzel, and E. Kruger. 2003. Inhibition of proteasome activity induces concerted expression of proteasome genes and de novo formation of mammalian proteasomes. *J. Biol. Chem.* **278**:21517–21525.
33. Penney, M., C. Wilkinson, M. Wallace, J. P. Javerzat, K. Ferrell, M. Seeger, W. Dubiel, S. McKay, R. Allshire, and C. Gordon. 1998. The Pad1+ gene encodes a subunit of the 26S proteasome in fission yeast. *J. Biol. Chem.* **273**:23938–23945.
34. Rao, H., F. Uhlmann, K. Nasmyth, and A. Varshavsky. 2001. Degradation of a cohesin subunit by the N-end rule pathway is essential for chromosome stability. *Nature* **410**:955–959.
35. Realini, C., C. C. Jensen, Z. Zhang, S. C. Johnston, J. R. Knowlton, C. P. Hill, and M. Rechsteiner. 1997. Characterization of recombinant REG $\alpha$ , REG $\beta$ , and REG $\gamma$  proteasome activators. *J. Biol. Chem.* **272**:25483–25492.
36. Rinaldi, T., C. Ricci, D. Porro, M. Bolotin-Fukuhara, and L. Frontali. 1998. A mutation in a novel yeast proteasomal gene, RPN11/MPR1, produces a cell cycle arrest, overreplication of nuclear and mitochondrial DNA, and an altered mitochondrial morphology. *Mol. Biol. Cell* **9**:2917–2931.
37. Rinaldi, T., R. Ricordy, M. Bolotin-Fukuhara, and L. Frontali. 2002. Mitochondrial effects of the pleiotropic proteasomal mutation mpr1/rpn11: uncoupling from cell cycle defects in extragenic revertants. *Gene* **286**:43–51.
38. Russell, S. J., S. H. Reed, W. Huang, E. C. Friedberg, and S. A. Johnston. 1999. The 19S regulatory complex of the proteasome functions independently of proteolysis in nucleotide excision repair. *Mol. Cell* **3**:687–695.
39. Rustgi, A. K. 2002. Securin a new role for itself. *Nat. Genet.* **32**:222–224.
40. Santamaria, P. G., D. Finley, J. P. Ballesta, and M. Remacha. 2002. Rpn6p, a proteasome subunit from *Saccharomyces cerevisiae*, is essential for the assembly and activity of the 26 S proteasome. *J. Biol. Chem.* **278**:6687–6695.
41. Schmid, I., C. H. Uittenbogaart, B. Keld, and J. V. Giorgi. 1994. A rapid method for measuring apoptosis and dual-color immunofluorescence by single laser flow cytometry. *J. Immunol. Methods* **170**:145–157.
42. Schwechheimer, C., and X. W. Deng. 2001. COP9 signalosome revisited: a novel mediator of protein degradation. *Trends Cell Biol.* **11**:420–426.
43. Shimanuki, M., Y. Saka, M. Yanagida, and T. Toda. 1995. A novel essential fission yeast gene pad1+ positively regulates pap1(+)-dependent transcription and is implicated in the maintenance of chromosome structure. *J. Cell Sci.* **108**:569–579.
44. Stitzel, M. L., R. Durso, and J. C. Reese. 2001. The proteasome regulates the UV-induced activation of the AP-1-like transcription factor Gcn4. *Genes Dev.* **15**:128–133.
45. Szlanka, T., L. Haraeska, I. Kiss, P. Deak, E. Kurucz, I. Ando, E. Viragh, and A. Udvardy. 2003. Deletion of proteasomal subunit S5a/Rpn10/p54 causes lethality, multiple mitotic defects and overexpression of proteasomal genes in *Drosophila melanogaster*. *J. Cell Sci.* **116**:1023–1033.
46. Unno, M., T. Mizushima, Y. Morimoto, Y. Tomisugi, K. Tanaka, N. Yasuoka, and T. Tsukihara. 2002. The structure of the mammalian 20S proteasome at 2.75 Å resolution. *Structure* **10**:609–618.
47. Ustrell, V., L. Hoffman, G. Pratt, and M. Rechsteiner. 2002. PA200, a nuclear proteasome activator involved in DNA repair. *EMBO J.* **21**:3516–3525.
48. Usui, T., M. Yoshida, A. Honda, T. Beppu, and S. Horinouchi. 1995. A K-252a-resistance gene, sks1+, encodes a protein similar to the *Caenorhabditis elegans* F37 A4.5 gene product and confers multidrug resistance in *Schizosaccharomyces pombe*. *Gene* **161**:93–96.
49. van Nocker, S., Q. Deveraux, M. Rechsteiner, and R. D. Vierstra. 1996. Arabidopsis MBP1 gene encodes a conserved ubiquitin recognition component of the 26S proteasome. *Proc. Natl. Acad. Sci. USA* **93**:856–860.
50. van Nocker, S., S. Sadis, D. M. Rubin, M. Glickman, H. Fu, O. Coux, I. Wefes, D. Finley, and R. D. Vierstra. 1996. The multiubiquitin-chain-binding protein Mcb1 is a component of the 26S proteasome in *Saccharomyces cerevisiae* and plays a nonessential, substrate-specific role in protein turnover. *Mol. Cell. Biol.* **16**:6020–6028.
51. Verma, R., L. Aravind, R. Oania, W. H. McDonald, J. R. Yates III, E. V. Koonin, and R. J. Deshaies. 2002. Role of Rpn11 metalloprotease in deubiquitination and degradation by the 26S proteasome. *Science* **298**:611–615.
52. Voges, D., P. Zwickl, and W. Baumeister. 1999. The 26S proteasome: a molecular machine designed for controlled proteolysis. *Annu. Rev. Biochem.* **68**:1015–1068.
53. Walz, J., A. Erdmann, M. Kania, D. Typke, A. J. Koster, and W. Baumeister. 1998. 26S proteasome structure revealed by three-dimensional electron microscopy. *J. Struct. Biol.* **121**:19–29.
54. Wilkinson, C. R., M. Penney, G. McGurk, M. Wallace, and C. Gordon. 1999. The 26S proteasome of the fission yeast *Schizosaccharomyces pombe*. *Philos. Trans. R. Soc. Lond. B* **354**:1523–1532.
55. Wilkinson, K. D. 2002. Cell biology: unchaining the condemned. *Nature* **419**:351–353.
56. Wojcik, C., and G. N. DeMartino. 2002. Analysis of *Drosophila* 26 S proteasome using RNA interference. *J. Biol. Chem.* **277**:6188–6197.
57. Xie, Y., and A. Varshavsky. 2001. RPN4 is a ligand, substrate, and transcriptional regulator of the 26S proteasome: a negative feedback circuit. *Proc. Natl. Acad. Sci. USA* **98**:3056–3061.
58. Yao, T., and R. E. Cohen. 2002. A cryptic protease couples deubiquitination and degradation by the proteasome. *Nature* **419**:403–407.
59. Young, P., Q. Deveraux, R. E. Beal, C. M. Pickart, and M. Rechsteiner. 1998. Characterization of two polyubiquitin binding sites in the 26S protease subunit 5a. *J. Biol. Chem.* **273**:5461–5467.
60. Zwickl, P. 2002. The 20S proteasome. *Curr. Top. Microbiol. Immunol.* **268**:23–41.